ISSN 2616-5767 Vol.6, Issue 12: 56-64, DOI: 10.25236/AJETS.2023.061209

Routing Optimization Model of Submarine Multi-beam Detection System Based on Trigonometric Function and Coordinate System

Zhuofan Zheng[1,a,*], Qirong Luo[1,b], Liga Wuri[1,c]

[1]Department of Electronic Information Engineering, North China University of Technology, Beijing, China
[a]15248588318@163.com, [b]18250567655@163.com, [c]17262670985@163.com
[*]Corresponding author

Abstract: *This paper establishes a mathematical model for the layout problem of the multibeam detection system in seabed exploration and analyzes the seabed detection problem from both two-dimensional and three-dimensional perspectives. Initially, utilizing trigonometric functions and the sine theorem, we calculate the water depth, coverage width, and coverage rate of the survey lines, formed by the tangent angles between the line spacing and the seabed depth. Subsequently, using a Cartesian coordinate system, we construct equations based on the relationships between vectors to compute the multibeam coverage width of survey lines at different distances from the center of the sea area. Under certain assumptions, we aim to cover the entire sea area with a minimal set of survey lines. Simplifying the seabed topography to two slopes of different gradients, we select contour lines formed by connecting two higher contour points to design the direction lines for the survey, thereby computing parameters such as the total length of the survey lines. This model is practical and effectively addresses the proposed issues, holding significance as a reference in the field of marine exploration.*

Keywords: *Multibeam Bathymetry, Trigonometric Functions, Three-Dimensional Slope Detection, Cartesian Coordinate System*

1. Introduction

The multibeam bathymetric system (MBES) is an acoustic device capable of conducting full-coverage seabed exploration, used for underwater terrain measurement and acquiring seafloor maps. Underwater terrain measurement generally involves two methods: single-beam bathymetric system and multibeam bathymetric system. The single-beam system utilizes the propagation characteristics of sound waves in water to measure water depth. The multibeam bathymetric system, developed based on the single-beam technology, emits tens to hundreds of beams in a plane perpendicular to the trajectory, simultaneously measuring a wider range of sea depths. Compared to single-beam systems, multibeam systems possess significant advantages in terms of data acquisition volume and efficiency. MBES is commonly employed in marine geology and geological exploration for mapping seafloor topography and structural addresses.

Researchers have focused on the processing methods of MBES data, with studies by Lurton and Lamarche [1, 2] exploring sonar echo data processing techniques. Simultaneously, breakthroughs have been achieved in the study of seafloor terrain features, such as Hughes Clarke [3] using MBES to study seamounts and crustal structures.Menna et al. [4] proposed a high-precision underwater archaeological site mapping method based on MBES. Additionally, research has been conducted on the application of MBES in marine environmental monitoring and infrastructure construction, with studies by Brown et al. [5] focusing on the study of seafloor ecosystems and Mayer [6, 7] researching the laying of underwater pipelines and cables.Hamden et al. [8] have discussed the development trends of multibeam bathymetric systems. Furthermore, Mitchell et al. [9] have studied the application of multibeam bathymetric systems in polar environments, while Wynn et al. [10] have focused on the application of multibeam bathymetric systems in deep-sea environments.

This paper primarily focuses on the layout problem of the multibeam detection system in seabed exploration. Taking into account the practical circumstances faced by the survey vessel in different sea areas, a mathematical model is established to address the problem, proposing different survey line

ISSN 2616-5767 Vol.6, Issue 12: 56-64, DOI: 10.25236/AJETS.2023.061209

designs and calculating related parameters.

2. Model establishment

2.1. Calculation Model of Multibeam Bathymetry in Two-Dimensional Seabed Profile

Due to the consistent slope of the seabed, the relationship between the difference in water depth at the center point and each survey line, as well as the distance between the survey lines and the center line, can be derived based on the properties of triangles such as the sine theorem and the angle theorem. Based on the relationship between water depth and coverage, the coverage width of each survey line is obtained. Finally, the overlap width is calculated based on the computed coverage width and the spacing of the survey lines and overlap rate between each survey line and the preceding one. The calculation parameters are represented as shown in Figure 1.

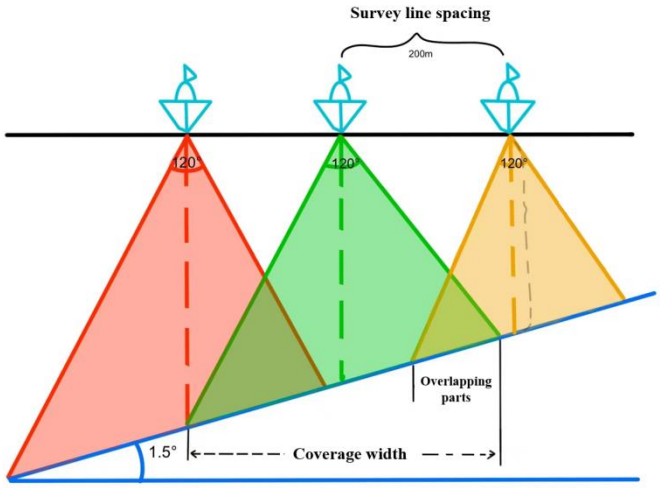

Figure 1: Cross-Section of Multiple Survey Lines

2.1.1. Calculation of Water Depth

The distance Δx from the survey line to the center point is a multiple of 200 meters. Due to the consistent slope of the seabed, based on the trigonometric theorem, the difference Δh between the water depth corresponding to each survey line and the water depth at the center point can be determined, with the ratio of the distance of each survey line from the center point being $tan\alpha$, as illustrated in Figure 2.

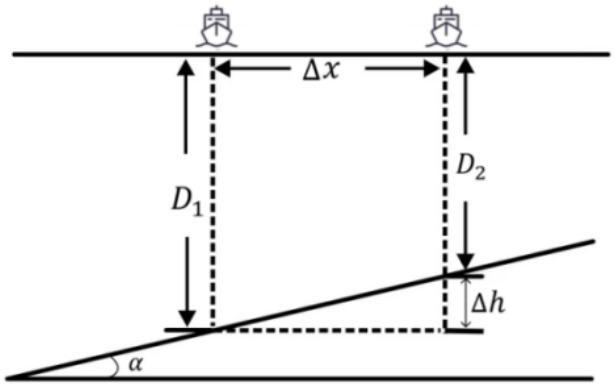

Figure 2: Sea Water Depth Calculation Model

According to the aforementioned geometric relationships, we can derive that:

$$\tan\alpha = \frac{\Delta h}{\Delta x} \tag{1}$$

ISSN 2616-5767 Vol.6, Issue 12: 56-64, DOI: 10.25236/AJETS.2023.061209

$$D_1 = D_2 + \Delta h = D_2 + \Delta x tan\alpha \tag{2}$$

Based on equations (1) and (2), we can obtain the water depth of all survey lines.

2.1.2. Calculation of Coverage Width

After modifying the above two-dimensional profile and adding auxiliary lines, the figure is shown in Figure 3.

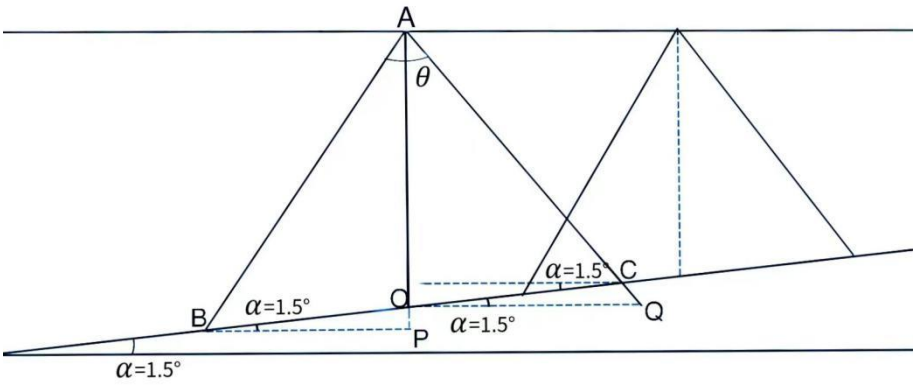

Figure 3: Simplified Calculation of Survey Plane

$$\frac{AO}{BO} = \frac{sin\angle ABO}{sin\angle OAB} \tag{3}$$

$$w = (BO + CO)cos\alpha \tag{4}$$

$$w = \mathrm{D} \times \left(\frac{sin\frac{\theta}{2}}{sin\left(90 + \alpha - \frac{\theta}{2}\right)} + \frac{sin\frac{\theta}{2}}{sin\left(90 - \alpha - \frac{\theta}{2}\right)} \right) cos\alpha \tag{5}$$

By substituting the result for the seabed depth D into equation (4), we can obtain all the required coverage widths.

2.1.3. Calculation of Adjacent Survey Line Coverage Rate

For this model's specific scenario, the adjacent survey line coverage rate is redefined as shown in Figure 4. Based on this definition, the overlap rate of the survey line with the preceding one in the figure is:

$$\text{Overlap rate} = \frac{\text{Overlapping part}}{\text{Coverage width}} \tag{6}$$

By constructing auxiliary lines based on the above image and annotating the points, we can draw a line parallel to the sea surface at point *B*, intersecting *A'B'* at point *P*. In parallelogram *AB A'B'*, *PB* = *A'A* = *d* due to the equality of angles θ in triangles *ABC* and *A'B'C'*. Furthermore, in the triangle *BPB'*, based on the sum of the interior angles being 180°, we have $\angle BPB' = 150°$ and $\angle PB'B = 28.5°$. Therefore, in triangle *BB'P*, we can use the sine theorem to obtain Figure 5.

ISSN 2616-5767 Vol.6, Issue 12: 56-64, DOI: 10.25236/AJETS.2023.061209

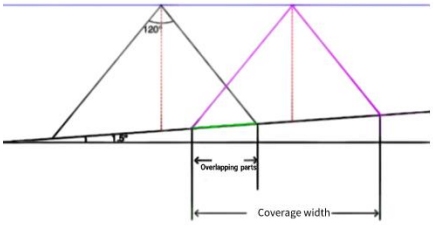

Figure 4: Definition of Overlap Rate

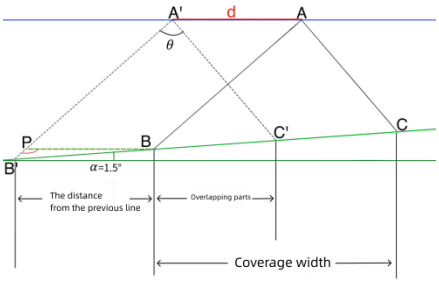

Figure 5: Overlap Rate Calculation

Suppose the remaining area of the preceding survey line is L, the coverage width of the preceding survey line is W_1, and the current survey line's coverage width is W_2, then we have:

$$\frac{BB'}{BP} = \frac{sin\angle BPB'}{sin\angle BB'P} \tag{7}$$

$$L = BB'\cos\alpha \tag{8}$$

$$\text{Overlap rate} = \frac{W_1 - L}{W_2} = \frac{W_1 - BB'\cos\alpha}{W_2} \tag{9}$$

Since the seabed slope remains constant, after calculating the corresponding coverage width using equation (4), we can substitute all the required points into equation (9).

2.2. Three-Dimensional Spatial Geometric Model

Assuming the survey ship is conducting exploration in a rectangular sea area with variable survey line directions, the multibeam transducer's opening angle is 120°, and the water depth at the center of the sea area is 120 meters. In this case, it is necessary not only to calculate the coverage width on the profile but also to determine the specific position of the survey line direction and coverage width. The establishment of a three-dimensional Cartesian coordinate system is used to determine the direction vector, the line-plane relationship, and the coverage width at different positions, as per the calculation equation (5). The three-dimensional seabed model is depicted in Figure 6.

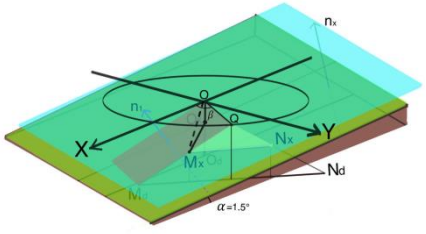

Figure 6: Three-dimensional Seabed Model

ISSN 2616-5767 Vol.6, Issue 12: 56-64, DOI: 10.25236/AJETS.2023.061209

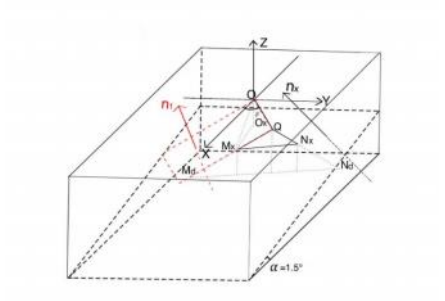

Figure 7: Schematic Diagram of the Model

In line with the above solution approach and the three-dimensional spatial view, we establish a three-dimensional Cartesian coordinate system with the projection of the seabed slope normal vector as the x-axis direction, the survey line direction as the positive y-axis direction at β=90°, and the upward direction at the center point as the positive z-axis direction, with the origin at the center of the sea area.

As shown in the figure 7, point O_x represents the projection point of the sea area center point on the seabed slope. Point Q represents the position of the survey ship, with the $\overrightarrow{OQ}$direction as the survey line direction. M_d and N_d are the points where the measurement beam can reach the farthest horizontal seabed plane, and M_x and N_x are the two farthest intersection points of the measurement beam with the seabed slope plane. Through the three-dimensional establishment, we can obtain the coordinates of point M_x using the following method:

Given $Q(xcos\beta, xsin\beta, 0)$, and since OM_x lies on the OQM_d plane and O_xM_x lies on the slope plane, three equations can be established with Q, M_x, and M_d being collinear. By solving the coordinates of point M through these three equations, we can obtain the result that the product of the plane vector and the normal vector is zero:

$$\begin{cases} \overrightarrow{OQ} \cdot \overrightarrow{n_1} = 0 \\ \overrightarrow{M_d} \cdot \overrightarrow{n_1} = 0 \end{cases} \tag{10}$$

The normal vector of the plane OQM_d plane is $\overrightarrow{n_1}$. According to the Angle of the submarine slope surface, the normal vector $\overrightarrow{n_x}$ of the slope surface can be directly written as ($tan\ a$, 0,1), and because the three lines of Q, M_x and M_d are collinear, $\overrightarrow{QM_x}$is proportional to $\overrightarrow{QM_d}$ abscissa, vertical coordinate and ordinate, so assume the coordinates of $\overrightarrow{M_x}$(a, b, c).

2.3. Survey Line Model in the Region with the Same Slope Angle

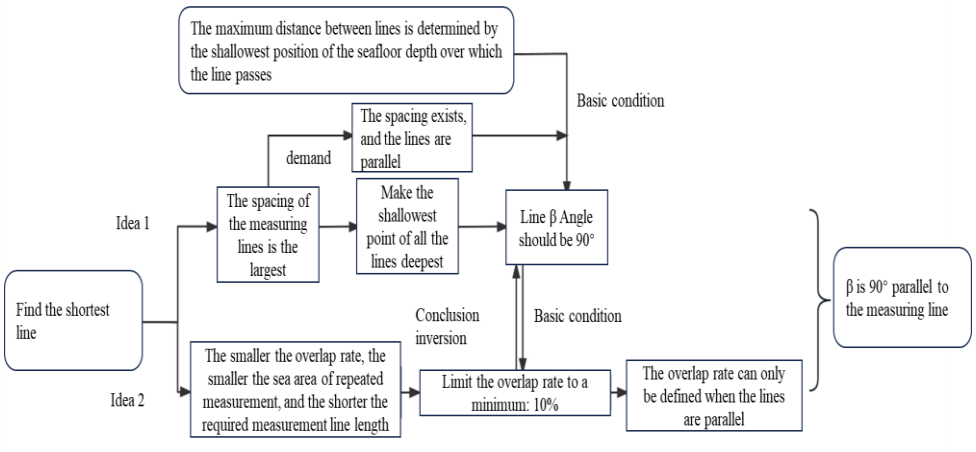

Figure 8: A flow chart for solving the total length of the measuring line

Suppose the survey ship is in a rectangular sea area with a length of 2 nautical miles from south to north and a width of 4 nautical miles from east to west. The water depth at the center of the sea area is

ISSN 2616-5767 Vol.6, Issue 12: 56-64, DOI: 10.25236/AJETS.2023.061209

110 meters, with the west being deeper than the east, and the seabed slope is 1.5°. The multibeam transducer has an opening angle of 120°. To ensure the coverage rate, the maximum distance between the survey lines should be determined by the shallowest position the survey lines pass through.

Simplify the problem by covering the entire area with strips, rotating the survey lines as a whole by β degrees, which is equivalent to maximizing the distance between the survey lines (Figure 8). The simplified problem is to determine the number of survey lines and the total length of the survey lines, with the constraint that the shallowest point overlap rate is 10% after fixing the angle for the group of survey lines. To ensure that the shallowest point each survey line passes through is as deep as possible, after calculating and analyzing, it is found that the optimal condition is β=90°, which means arranging all the survey lines vertically. Furthermore, to reduce the number of survey lines and increase the width between them, it is advisable to constrain the overlap rate to 10% considering that the overlap rate is between 10% and 20%. Therefore, expanding equation (9), we obtain:

$$\eta(\mathrm{x})=\frac{W(x-d)-\dfrac{d\cdot sin\left(90^{\circ}+\dfrac{\theta}{2}\right)\cos\alpha}{sin\left(90^{\circ}-\alpha-\dfrac{\theta}{2}\right)}}{W(x)}=\frac{W(x-d)}{W(x)}-\frac{d\cdot sin\left(90^{\circ}+\dfrac{\theta}{2}\right)\cos\alpha}{sin\left(90^{\circ}-\alpha-\dfrac{\theta}{2}\right)W(x)} \quad (11)$$

At this point, the distance d between the survey lines, where x is the current distance of the survey line from the center of the sea area, and x-d represents the distance between the previous survey line and the center point. By adjusting d to ensure that η(x) = 10%, it is possible to directly calculate the distance d between each survey line and the preceding one.

2.4. Complex Survey Line Optimization Model

Based on the seabed depth data computed using the single-beam survey lines. According to the analysis process in section 2.3, when the angle β between the survey line direction and the normal projection direction of the seabed surface is 90°, the shortest survey lines can be obtained. By observing the visualized data, the seabed can be roughly divided into two slopes: a steep slope *DBB'* and a gentle slope *AB'B*. With a fixed overlap rate for multibeam detection, the deeper the seabed, the larger the distance between the survey lines.

2.4.1. Model Simplification

For this complex model, it can be simplified as shown in Figure 9. It can be observed that *EF* is in a constant proportion to *AB* when the overlap rate is constant, while *AB*, representing the known distance between the survey lines, is in proportion to *HI*. Thus, it can be noted that the deeper the seabed, the larger the distance between the survey lines, as illustrated in Figure 10.

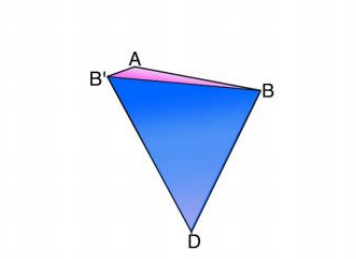

Figure 9: Schematic of the Simplified Survey Line Model

ISSN 2616-5767 Vol.6, Issue 12: 56-64, DOI: 10.25236/AJETS.2023.061209

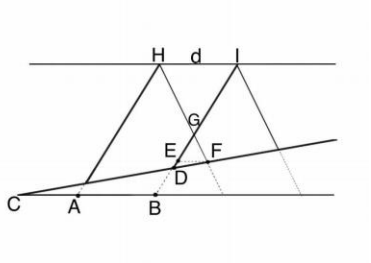

Figure 10: Relationship between Overlap Rate and Survey Line Spacing

Regarding the selection of the dividing lines between the two slopes, there are two options: the line connecting *B* and the contour point *B'* at *x*=0, and the line connecting *C* and the contour point *C'* at *x*=4, *y*=5. Considering that the shallower regions correspond to larger inter-line spacing for the same overlap rate, and the overall height of line *CC'* is higher than that of line *BB'*, it follows that line *BB'* is deeper compared to line *CC'*. Therefore, *BB'* is ultimately chosen as the dividing line between the two planes to increase the spacing between the lateral lines and thus reduce the total length of the survey lines.

2.4.2. Model Solution and Analysis

Based on the schematic diagram, the slope angle α can be easily determined. After calculating the slope angle α, the final survey line diagram can be obtained using the method outlined in section 2.3.For the calculation of the plane slope angle after selecting *BB'* as the dividing line, refer to Figure 11.

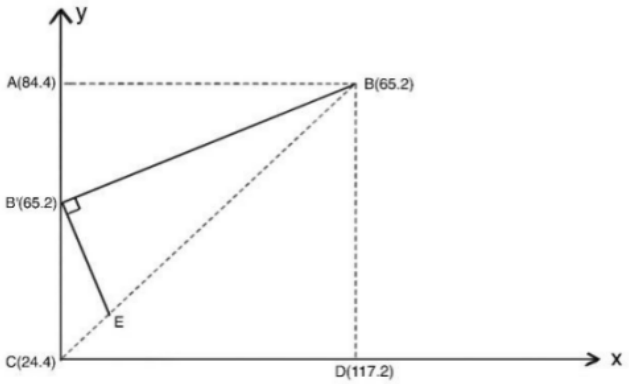

Figure 11: Slope Angle Solution

$$BE = \frac{BB'}{cos\angle EBB'} \tag{12}$$

$$\angle EBB' = \angle CBA - \angle B'BA \tag{13}$$

$$\angle CBA = tan^{-1}\frac{CA}{AB} \tag{14}$$

$$\angle B'BA = tan^{-1}\frac{B'A}{AB} \tag{15}$$

From the above equations, we can calculate $\angle EBB'$. After obtaining $\angle EBB'$, we can find *BE* and *B'E*. With these two values, we can use the arctan function to calculate the slope angle.

3. Results

For the sea water depth at different distances from the center of the sea area, the coverage width of the multibeam, and the coverage rate with the preceding survey line, the results are shown in Table 1.

ISSN 2616-5767 Vol.6, Issue 12: 56-64, DOI: 10.25236/AJETS.2023.061209

Table 1: Sea Water Depth, Coverage Width, and Overlap Rate at Different Distances

Distance of the survey line from the center point/m	-800	-600	-400	-200	0	200	400	600	800
Sea water depth/m	90.94873726	85.71155294	80.47436863	75.23718431	70	64.76281569	59.52563137	54.28844706	49.05126274
Coverage width/m	315.70510695	297.52557105	279.34603515	261.16649926	242.98696336	224.80742746	206.62789156	188.44835566	170.26881976
Overlap rate with the previous survey line/%	—	35.695443	31.510572	26.743092	21.262236	14.894938	7.407224	-1.525164	-12.364966

Using equation (5) for verification, at the center point with a seabed depth of 120m and a lateral line direction of 90°, the calculated coverage width is W=416.54908m, which matches the previous result, confirming the accuracy of the calculations. The results obtained from the survey line model are shown in Table 2.

Table 2: Results Obtained from the Survey Line Model

East-West coordinates	Survey line	East-West coordinates	Survey line	East-West coordinates	Survey line	East-West coordinates	Survey line
0	-3851	**11**	848	**22**	2735	**33**	3560
1	-3222	**12**	1091	**23**	2841	**34**	3606
2	-2642	**13**	1316	**24**	2939	**35**	3649
3	-2108	**14**	1525	**25**	3030	**36**	3689
4	-1615	**15**	1719	**26**	3115	**37**	3726
5	-1161	**16**	1899	**27**	3194		
6	-742	**17**	2066	**28**	3267		
7	-356	**18**	2221	**29**	3335		
8	0	**19**	2364	**30**	3398		
9	304	**20**	2497	**31**	3456		
10	586	**21**	2620	**32**	3510		

Since the model is based on a 10% coverage rate limit, the above survey lines may extend beyond the sea area, but they will be considered in the total length calculation. According to the survey lines described above, the total distance is calculated to be 140752m.

In the complex survey line optimization model, the slope angle r is calculated to be 0.39983871280891276. This value can be used to compute the intersection points of each survey line with the y-axis. Additionally, given that $\angle B'BA$ = 21.80140948635182, the total length of the survey lines can be calculated to be 573771.1610152135m. The estimated proportion of the total length occupied by the part where the overlap rate exceeds 20% is approximately 30%, while the area of the sea left uncovered can be considered negligible.

Simultaneously, we compare different survey line optimization models to highlight the advantages of our proposed method. We contrast our approach with other common survey line optimization models, such as the genetic algorithm-based optimization model and the greedy algorithm-based optimization model. Although genetic algorithms have achieved success in many optimization problems, their computation time is relatively long. Our method, based on trigonometric functions and coordinate system construction, is intuitive and computationally efficient, allowing for satisfactory solutions in a shorter time. As for the greedy algorithm, it may fall into local optima; however, our method considers satisfying the overlap rate of adjacent bands when designing survey lines, possessing stronger global optimization capabilities, and thus finding better solutions.

4. Conclusion

This article proposes a model for the measurement lines of a multibeam depth sounding system based on trigonometric functions. The model employs a simplified approach, capturing the essential factors influencing the measurement problem. By transforming the complex problem into a straightforward mathematical model, it becomes intuitive, easy to comprehend, and exhibits high accuracy. The derivation of the model is based entirely on trigonometric relationships, ensuring clarity

ISSN 2616-5767 Vol.6, Issue 12: 56-64, DOI: 10.25236/AJETS.2023.061209

and a broad applicability range.

In summary, our approach has significant advantages in practicality, algorithm intuitiveness, and fully considering seabed terrain and coverage. Compared to other methods, our approach is better suited to address the challenges of the actual marine detection field, providing an effective solution for optimizing the wiring of underwater multibeam detection systems.

References

[1] Lurton, X. (2010). An introduction to underwater acoustics: principles and applications. Springer Science & Business Media.https://doi.org/10.1007/978-3-642-13835-5

[2] Lamarche, G., & Lurton, X. (2015). Quantitative characterisation of seafloor substrate and bedforms using advanced processing of multibeam backscatter—Application to Cook Strait, New Zealand. Continental Shelf Research, 105, 6-24.https://doi.org/10.1016/j.csr.2010.06.001

[3] Hughes Clarke, J. E. (2016). First wide-angle view of channelized turbidity currents links migrating cyclic steps to flow characteristics. Nature Communications, 7, 11896.https://doi.org/ 10.1038/ ncomms11896

[4] Menna, F., Nocerino, E., Troisi, S., & Remondino, F. (2013, May). A photogrammetric approach to survey floating and semi-submerged objects. In Videometrics, Range Imaging, and Applications XII; and Automated Visual Inspection (Vol. 8791, pp. 117-131). SPIE.https://doi.org/10.1117/12.2020464

[5] Brown, C. J., Smith, S. J., Lawton, P., & Anderson, J. T. (2011). Benthic habitat mapping: A review of progress towards improved understanding of the spatial ecology of the seafloor using acoustic techniques. Estuarine, Coastal and Shelf Science, 92(3), 502-520.https://doi.org/ 10.1016/j. ecss. 2011.02.007

[6] Mayer, L. A. (2006). Frontiers in seafloor mapping and visualization. Marine Geophysical Research, 27(1), 7-17.https://doi.org/10.1007/s11001-005-0267-x

[7] Pirenne, B., Mayer, L. A., & Hughes Clarke, J. E. (2015). Multibeam sonar backscatter data processing. In Seafloor Mapping Along Continental Shelves (pp. 153-175). Springer, Cham.https://doi. org/ 10. 1007/s11001-018-9341-z

[8] Hamden, M. H., & Md Din, A. H. (2018, July). A review of advancement of hydrographic surveying towards ellipsoidal referenced surveying technique. In IOP Conference Series: Earth and Environmental Science (Vol. 169, p. 012019). IOP Publishing.

[9] Mitchell, G. A., Orange, D. L., Gharib, J. J., & Kennedy, P. (2018). Improved detection and mapping of deepwater hydrocarbon seeps: Optimizing multibeam echosounder seafloor backscatter acquisition and processing techniques. Marine Geophysical Research, 39, 323-347.https://doi. org/10. 1007/s11001-018-9345-8

[10] Wynn, R. B., Huvenne, V. A., Le Bas, T. P., Murton, B. J., Connelly, D. P., Bett, B. J., ... & Morris, K. J. (2014). Autonomous Underwater Vehicles (AUVs): Their past, present and future contributions to the advancement of marine geoscience. Marine Geology, 352, 451-468.https://doi. org/10. 1016/j. margeo. 2014.03.012